Nontrivial Fixed Point in a Twofold Orbitally Degenerate Anderson Impurity Model

Michele Fabrizio,[1,2] Andrew F. Ho,[3] Lorenzo De Leo,[1] and Giuseppe E. Santoro[1,2,4]

[1]*International School for Advanced Studies (SISSA), and Instituto Nazionale per la Fisica della Materia (INFM) UR-Trieste SISSA, Via Beirut 2-4, I-34014 Trieste, Italy*

[2]*The Abdus Salam International Centre for Theoretical Physics (ICTP), P.O. Box 586, I-34014 Trieste, Italy*

[3]*School of Physics and Astronomy, The University of Birmingham, Edgbaston, Birmingham B15 2TT, United Kingdom*

[4]*INFM Democritos National Simulation Center, Via Beirut 2-4, I-34014 Trieste, Italy*

(Received 19 May 2003; published 10 December 2003)

We study a twofold orbitally degenerate Anderson impurity model which shows a nontrivial fixed point similar to that of the two-impurity Kondo model, but remarkably more robust, as it can only be destabilized by orbital- or gauge-symmetry breaking. The impurity model is interesting per se, but here our interest is rather in the possibility that it might be representative of a strongly correlated *lattice* model close to a Mott transition. We argue that this lattice model should unavoidably encounter the nontrivial fixed point just before the Mott transition and react to its instability by spontaneous generation of an orbital, spin-orbital or superconducting order parameter.

DOI: 10.1103/PhysRevLett.91.246402 PACS numbers: 71.30.+h, 71.10.–w, 72.15.Qm, 72.15.Rn

When a metal is driven by strong correlations towards a Mott insulator, an incoherent component of the single-particle spectrum slowly moves away from the quasiparticle resonance and smoothly transforms into the Mott-Hubbard sidebands. Analogous behavior is displayed by an Anderson impurity model (AIM) from the mixed valence to the Kondo regime. This is suggestive of similar physical processes underlying the dynamics of AIM's and of strongly correlated electron systems across the Mott metal-to-insulator transition (MIT), even though a rigorous relationship holds only in infinite dimensions, as shown by dynamical mean field theory (DMFT). Furthermore, DMFT shows that the Mott-Hubbard bands split off from the quasiparticle resonance quite before the MIT occurs [1], suggesting that it is rather the physics of the AIM in the Kondo regime to be significant near the MIT. In that limit, the AIM maps onto a Kondo model with the number of conduction channels always such as to *perfectly* screen the impurity. For that reason one would exclude that the appealing non-Fermi liquid physics of the *overscreened* multichannel Kondo effect may ever appear close to the MIT.

That expectation is partly wrong. In this Letter we study the phase diagram of an AIM which does contain a nontrivial fixed point. We show that the physical behavior around this fixed point resembles that displayed by the two-impurity Kondo model. We also argue that the lattice model, where the physics of the above AIM should be relevant, necessarily encounters this fixed point just before the MIT, and discuss possible consequences.

We consider the two-orbital AIM Hamiltonian:

$$\hat{H}_{\rm AIM} = \sum_{k,a,\sigma} [\epsilon_k\, c^\dagger_{k,a\sigma} c_{k,a\sigma} + (V_k c^\dagger_{k,a\sigma} d_{a\sigma} + \text{H.c.})] + \frac{U}{2}(n_d - 2)^2 + \hat{H}_K, \quad (1)$$

where $c^\dagger_{k,a\sigma}$ are conduction-band creation operators in orbital $a = 1, 2$ and spin σ, $d^\dagger_{a\sigma}$ impurity ones and $n_d = \sum_{a\sigma} d^\dagger_{a\sigma} d_{a\sigma}$. For $\hat{H}_K = 0$, the AIM has a large SU(4) symmetry which is lowered down to a spin SU(2) times an orbital O(2) by a Hund's rule-like coupling:

$$\hat{H}_K = K[(\hat{T}^x)^2 + (\hat{T}^y)^2], \quad (2)$$

where $\hat{T}^i = \frac{1}{2}\sum_\sigma \sum_{a,b=1}^2 d^\dagger_{a\sigma}\, \tau^i_{ab}\, d_{b\sigma}$, $i = x, y, z$, are orbital pseudospin operators with τ^i's the Pauli matrices. For later convenience, we also introduce the impurity spin, $\hat{S}^i = \frac{1}{2}\sum_a \sum_{\alpha,\beta} d^\dagger_{a\alpha}\, \sigma^i_{\alpha\beta}\, d_{a\beta}$, and the impurity spin-orbital operators $\hat{W}^{ij} = \frac{1}{2}\sum_{a,b} \sum_{\alpha,\beta} d^\dagger_{a\alpha}\, \sigma^i_{\alpha\beta}\, \tau^j_{ab} d_{b\beta}$.

In the Kondo regime, U much larger than the conduction bandwidth, two electrons get trapped by the impurity in a configuration identified by total spin, S, total pseudospin, T, and their z components, with energy $E(S, S^z; T, T^z) = K[T(T+1) - (T^z)^2]$. By Pauli principle, two electron configurations have either $S = 1$ and $T = 0$, or $S = 0$ and $T = 1$. If $K > 0$, the lowest energy configuration has $S = 1$ and $T = 0$, the conventional Hund's rules. The impurity behaves effectively as a spin $S = 1$ which may be Kondo screened by the two conduction channels ($\delta = \pi/2$ phase shift). On the contrary, if $K < 0$ the nondegenerate $S = 0$ $T = 1$ and $T^z = 0$ state has lowest energy. Here we do not expect any Kondo effect, i.e., $\delta = 0$. This situation is analogous to the two $S = 1/2$ impurity Kondo model (2IKM) in the presence of a direct exchange between the impurities. There, it is known [2–4] that under particular circumstances an unstable fixed point (UFP) separates the Kondo-screened regime from the one in which the two-impurities couple together into a singlet. In our model (1), that circumstance is realized thanks to the O(2) orbital symmetry, as shown later, hence an analogous UFP should exist.

We have studied the AIM (1) in the Kondo regime by Wilson's numerical renormalization group (NRG), closely following the original work by Jones and Varma

for the 2IKM [2,4]. We have also developed a complementary analysis based on Abelian bosonization, which provides a better characterization of the UFP.

In the inset of Fig. 1 we sketch the phase diagram of (1) in the Kondo regime, as determined by the flow of the low-energy spectrum obtained by NRG. At fixed Kondo exchange we find indeed an UFP upon varying K. For $K > K_*$, the model asymptotically flows to a Kondo-screened fixed point, see right panel in Fig. 1, while for $K < K_* < 0$ it flows towards a non-Kondo-screened fixed point, see left panel. The intermediate crossover region, also shown in Fig. 1, identifies the UFP [5]. We notice that (1) has a larger impurity Hilbert space than the 2IKM, which contains, besides the $S = 1$ and the $T^z = 0$ $S = 0$ configurations, also the $T^z = \pm 1$ $S = 0$ doublet, absent in the 2IKM. In spite of that, the low-energy spectra at the UFP's are the same for both models. In Fig. 2 we plot the ground state average values of the impurity operators $\vec{S}^2$, $\vec{T}^2$, and $(T^z)^2$. For large and positive K, the impurity freezes into the $S = 1$ $T = 0$ configuration while, for very negative values, into the $T^z = 0$ $S = 0$ one. At the UFP $\langle S^2 \rangle = 1/2$, $\langle T^2 \rangle = 3/2$, and $\langle (T^z)^2 \rangle = 1/4$. To prove that our UFP is connected with the 2IKM one, we have added to (1) a term $G_z(\hat{T}^z)^2$, with $G_z > 0$, which pushes upward the energy of the $T^z = \pm 1$ $S = 0$ doublet absent in the 2IKM. In the inset of Fig. 2 we plot $\langle S^2 \rangle$ as function of G_z at the UFP, whose position depends on G_z too. We do find that $\langle S^2 \rangle$ smoothly reaches the 2IKM unit value for large G_z.

The approach to the two stable fixed points, $K < K_*$ and $K > K_*$, can be described by the local perturbation left behind by the impurity which has either disappeared, $\delta = 0$, or been absorbed by the conduction sea, $\delta = \pi/2$:

$$\hat{H}_* = -\sum_{a\sigma} t_* (f^\dagger_{0,a\sigma} f_{1,a\sigma} + \text{H.c.}) + \frac{U_*}{2}(n_0 - 2)^2 + J_{S*}\vec{S}_0 \cdot \vec{S}_0 + J_{T*}(\hat{T}^z_0)^2, \quad (3)$$

where "0" labels the first available site of the Wilson chain, i.e., the actual first site for $K < K_*$, $\delta = 0$, and the second site for $K > K_*$, $\delta = \pi/2$. Numerically we find $J_{T*} \sim 2U_* \sim 2J_{S*} \sim 32 t_* \to \infty$ upon approaching the UFP, see Fig. 3. The diverging t_* implies a singular $[\propto (K - K_*)^{-2}]$ impurity contribution to the specific heat, just as in the 2IKM. Additional information is provided by the Wilson ratios $R_i = (c_v\, \delta\chi_i)/(\chi_i\, \delta c_v)$, where $i = S, T^z$ refer to spin and orbital susceptibilities, i.e., to those response functions which are related to conserved quantities and, hence, are accessible by Fermi liquid theory [6,7]. R_S and R_{T^z} are shown in Fig. 4 and appear to vanish at the UFP. By analogy with the 2IKM, there are two other susceptibilities which are instead expected to be singular: the susceptibility χ_{ST^z} to a field which couples to the relative spin operator $\hat{W}^{iz}$, $i = x, y, z$ (the staggered spin-susceptibility in the 2IKM), and the pairing susceptibility χ_{SC} in the Cooper

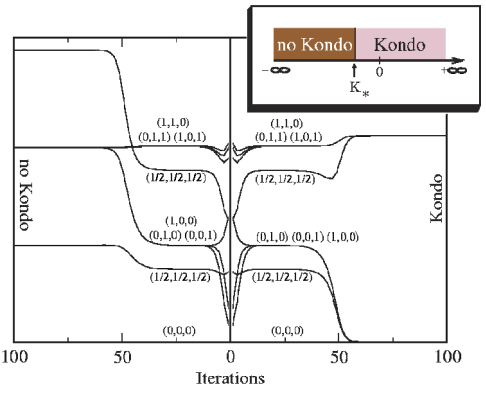

FIG. 1 (color online). NRG flow of the lowest energies of the levels labeled by (Q, T^z, S), where Q is half of the added charge. The right and left flows correspond to a relative deviation $\delta K_*/K_* = \pm 4 \times 10^{-3}$ from the fixed point value K_*, respectively. The phase diagram is sketched in the inset.

channel $c^\dagger_{1\uparrow} c^\dagger_{2\downarrow} + c^\dagger_{2\uparrow} c^\dagger_{1\downarrow}$. Those are not accessible by Fermi liquid theory. Yet one can get a rough estimate of them by the corresponding scattering amplitudes at zero external frequencies. They are given, respectively, by $\Gamma_{ST^z} = -2U_* + J_{S*} - J_{T*}$ and $\Gamma_{SC} = 2U_* - 3J_{S*} - J_{T*}$, and hence are negative (corresponding to an enhancement of the response) and diverge similarly approaching the UFP. The physics underneath is the same of the 2IKM, and has been exhaustively discussed in Ref. [4]. The UFP has a residual entropy $\ln\sqrt{2}$. Away from the UFP, this entropy is quenched below a temperature scale $T_* \sim |K - K_*|^2$, implying a specific heat coefficient $\gamma \sim 1/T_*$. The rest of the impurity entropy is quenched at higher temperatures of order $T_K \sim |K|$. At the UFP, γ is finite, while both χ_{ST^z} and χ_{SC} display a $|\ln T|$ singularity.

The stability of the UFP is more easily accessed by Abelian bosonization, following Ref. [8] on the 2IKM. In the large U limit, (1) maps onto the Kondo model

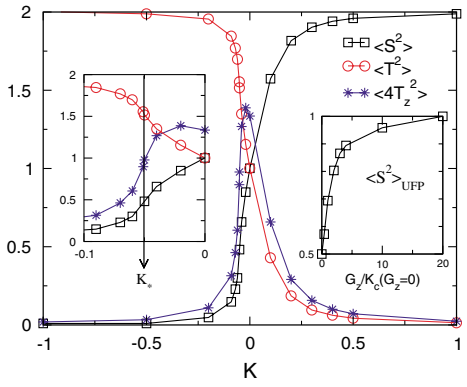

FIG. 2 (color online). Average impurity quantum numbers as function of K. In the left inset the behavior around the UFP is shown in more detail, while in the right inset $\langle S^2 \rangle$ along the path towards the 2IKM is displayed (see text).

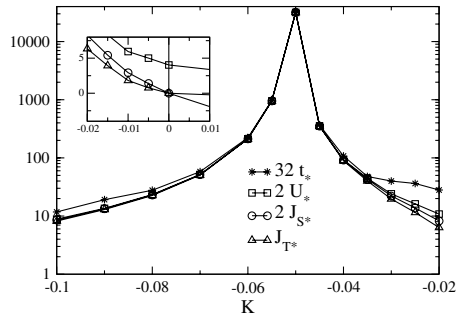

FIG. 3. K dependence of the effective couplings in Eq. (3). In the inset the region around $K = 0$ is shown.

$$\hat{H}_{s-d} = \sum_{k,a,\sigma} \epsilon_k c^\dagger_{k,a\sigma} c_{k,a\sigma} + \hat{H}_K + \sum_{i,j=1}^{3} J_W^{ij} \hat{W}^{ij} \hat{\omega}^{ij} + \sum_{i=1}^{3} (J_S^i \hat{S}^i \hat{\sigma}^i + J_T^i \hat{T}^i \hat{\tau}^i), \quad (4)$$

where $\hat{\sigma}^i$, $\hat{\tau}^i$, and $\hat{\omega}^{ij}$ are, respectively, the conduction-electron spin, orbital, and spin-orbital densities at the impurity site. As usual in Abelian bosonization we allow for anisotropy: $J_S^x = J_S^y \neq J_S^z$, and similarly for J_T^i and J_W^{ij}. We further assume $J_W^{ij} = J_W^\perp$, for $i, j \neq z$. The anisotropic Kondo model (4) has a continuous $O(2)_{\text{spin}} \times O(2)_{\text{orbital}} \times U(1)_{\text{charge}}$ symmetry, which is useful to decompose into $U(1)_{\text{spin}} \times U(1)_{\text{orbital}} \times U(1)_{\text{charge}}$ plus two discrete symmetries: (i) a Π_x^{spin} rotation: $c_{a,\sigma} \leftrightarrow c_{a,-\sigma}$ and $d_{a,\sigma} \leftrightarrow d_{a,-\sigma}$; and (ii) a Π_x^{orb} rotation: $c_{1\sigma} \leftrightarrow c_{2\sigma}$ and $d_{1\sigma} \leftrightarrow d_{2\sigma}$. By Abelian bosonization [9], we write the s-wave scattering components of conduction electrons as chiral one-dimensional fermions $c_{a,\sigma}(x) = 1/\sqrt{2\pi\alpha}\, F_{a,\sigma} \exp[-i\phi_{a,\sigma}(x)]$, where $\phi_{a,\sigma}$ are chiral free Bose fields, α a short distance cutoff, and the Klein factors $F_{a,\sigma}$ are Grassman variables enforcing proper anticommutation relations. Next, we introduce the combinations: $\phi_c = (\phi_{1\uparrow} + \phi_{1\downarrow} + \phi_{2\uparrow} + \phi_{2\downarrow})/2$, $\phi_s = (\phi_{1\uparrow} - \phi_{1\downarrow} + \phi_{2\uparrow} - \phi_{2\downarrow})/2$, $\phi_f = (\phi_{1\uparrow} + \phi_{1\downarrow} - \phi_{2\uparrow} - \phi_{2\downarrow})/2$, $\phi_{sf} = (\phi_{1\uparrow} - \phi_{1\downarrow} - \phi_{2\uparrow} + \phi_{2\downarrow})/2$. After applying the canonical transformation $\exp[i\hat{S}^z\phi_s(0)] \times \exp[i\hat{T}^z\phi_f(0)]$, Eq. (4) can be refermionized via $\Psi_b(x) = 1/\sqrt{2\pi\alpha}\, F_b \exp[-i\phi_b(x)]$, where $b = c, s, f, sf$ [9]. For a particular value of $J_S^z = J_T^z$, the end result is an effective model where only Ψ_{sf} is coupled to the impurity, just as in the 2IKM [8].

To locate the UFP, we follow the same strategy of Ref. [8]: we assume K large compared to the conduction bandwidth and search for an accidental ground state degeneracy in that part of the effective Hamiltonian involving just the impurity and the F_b's:

$$\hat{H}_{\text{imp}} = \hat{H}_K + \lambda_S(\hat{S}^z)^2 + \lambda_T(\hat{T}^z)^2 + \frac{J_W^\perp}{2\pi\alpha}[F_s^\dagger F_f^\dagger \hat{W}^{--} + F_f F_s^\dagger \hat{W}^{-+} + \text{H.c.}]. \quad (5)$$

λ_S and λ_T are cutoff dependent functions of J_S^z, J_T^z. For a specific $K_* < 0$, we find that the impurity state $|0\rangle \equiv |S = 0, S^z = 0; T = 1, T^z = 0\rangle$ is degenerate with:

$$|1\rangle \equiv \frac{\cos\theta}{\sqrt{2}}(F_f\ |0, 0; 1, +1\rangle + F_f^\dagger\ |0, 0; 1, -1\rangle) + \frac{\sin\theta}{\sqrt{2}}(F_s\ |1, +1; 0, 0\rangle - F_s^\dagger\ |1, -1; 0, 0\rangle), \quad (6)$$

where θ depends on the Hamiltonian parameters. For our model (1), θ should be equal to $\pi/4$ to reproduce the observed UFP average values of S^2, T^2, and $(T^z)^2$. If we added the term $G_z\,(\hat{T}^z)^2$, θ should increase with G_z, reaching the 2IKM value of $\theta = \pi/2$ for large G_z. The Klein factors in (6) show that $|0\rangle$ and $|1\rangle$ differ by one fermion, justifying the introduction of a fictitious fermion connecting that doublet: $f^\dagger\ |0\rangle = \ |1\rangle$.

The low-energy Hamiltonian close to the UFP, $\hat{H}_{\text{UFP}}$, is then obtained by projection onto the above doublet-subspace. Including up to dimension 3/2 operators,

$$\hat{H}_{\text{UFP}} = H_0 + \lambda_0[\Psi_{sf}^\dagger(0) - \Psi_{sf}(0)](f^\dagger + f) + \lambda_1 \partial_x[\Psi_{sf}^\dagger(0) - \Psi_{sf}(0)](f^\dagger - f) + \delta K_* f^\dagger f, \quad (7)$$

with H_0 the free Hamiltonian for the $\Psi_b(x)$'s, and δK_* the deviation from the fixed-point value K_*. λ_0 and λ_1 are model dependent parameters. As expected, Eq. (7) has the same form as in the 2IKM [8]. The UFP Hamiltonian [first line of Eq. (7)] is a resonant level model involving one Majorana fermion $\Psi_{sf}^\dagger - \Psi_{sf}$ hybridizing with $f^\dagger + f$. The combination $f^\dagger - f$ is free and is responsible for the $\ln\sqrt{2}$ UFP residual entropy. The relevant term (dimension 1/2) proportional to δK_* describes the deviation from the UFP, while the λ_1 term is the leading irrelevant operator (dimension 3/2). Other possibly relevant operators are instead not allowed by the symmetry properties of (4), which have to be preserved by $\hat{H}_{\text{UFP}}$ too. For instance, among the particle-hole symmetry breaking terms allowed in the 2IKM [4], only the marginal one, which does not spoil the UFP properties, may appear in our model, since the relevant operator, bosonization of which is given by $[\Psi_f^\dagger(0) + \Psi_f(0)](f - f^\dagger)$ [8], is here forbidden by $U(1)_{\text{orbital}}$. In fact, while f is invariant under a $U(1)_{\text{orbital}}$ rotation parametrized by a phase α, due to the Klein factors in (6), Ψ_f transforms into $e^{2i\alpha}\Psi_f$. Indeed all relevant perturbations which destabilize the UFP correspond to physical instabilities of model (1), unlike what happens in the 2IKM. For instance, the relevant terms $[\Psi_c(0) \pm \Psi_c^\dagger(0)](f - f^\dagger)$, of dimension 1/2, break $U(1)_{\text{charge}}$. Therefore, gauge-symmetry breaking destabilizes the UFP, which explains the singular behavior of χ_{SC}. Analogously, χ_{ST^z} is the response to a field which breaks $SU(2)_{\text{spin}} \times \Pi_x^{\text{orb}}$ and allows the relevant terms [10] $[\Psi_{\text{sf}}^\dagger(0) + \Psi_{\text{sf}}(0)](f - f^\dagger)$ [4,8] and $[\Psi_s^\dagger(0) \pm \Psi_s(0)](f - f^\dagger)$. Besides those two susceptibilities, also

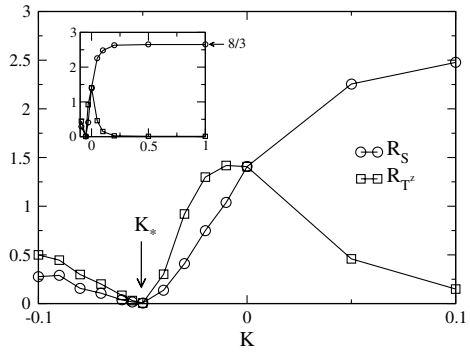

FIG. 4. Spin (R_S) and orbital (R_{T^z}) Wilson ratios as functions of K. Notice that the $K = 0$, SU(4)-point, as well as large K, $S = 1$ impurity (shown in the inset), values coincide with known results.

χ_{T^a} and χ_{ST^a}, with $a = x, y$, are logarithmically diverging, being related to fields breaking $\mathrm{U}(1)_{\mathrm{orbital}}$.

We now turn to our original motivation and discuss the possible relevance of the above results to the physics of the Mott transition. Take a lattice model with an on-site interaction of the same form as in (1) and (2), with inverted Hund's coupling $K < 0$. This may occur if the electrons are Jahn-Teller coupled to two degenerate weakly dispersive optical phonons by $g\sum_R(q_{1R}\hat{T}^x_R + q_{2R}\hat{T}^y_R)$, where q_{iR} are the phonon coordinates on-site R. This coupling gives rise to a retarded electron-electron interaction which reduces to (2) with $K \simeq -g^2/\omega_0$ when the typical phonon frequency ω_0 is much larger than the quasiparticle bandwidth. Alternatively, two single-band Hubbard planes/chains coupled by $J\sum_R \vec{S}_{1R} \cdot \vec{S}_{2R}$, where 1 and 2 refer to the two planes/chains and $J > 0$, would also display a similar behavior.

When $K = 0$ the lattice model should undergo a MIT at some finite U_c in the absence of nesting. If $|K| \ll U_c$, the physics of the metallic phase near the MIT should resemble that of the AIM, Eq. (1), in the Kondo regime. Since the width of the quasiparticle resonance, i.e., the effective Kondo temperature T_K, vanishes at the MIT, $T_K \sim U_c - U$ [1], the system is forced to enter the critical region around the unstable fixed point, $|K| \sim T_K$, before the MIT occurs. However, the instability of the AIM around the UFP towards the orbital O(2) or charge U(1) symmetry breakings should transform in the lattice model into a true bulk instability. Namely, at least within DMFT, we expect that the self-consistency condition which relates the impurity Green's function with the local Green's function of the bath enlarges the UFP into a whole region where the model undergoes a spontaneous symmetry breaking. This would open up new screening channels for those degrees of freedom which survive below T_K down to $T_* \sim |T_K + K|^2/T_K$ ($K < 0$) and are responsible of the finite entropy at the UFP. If the band structure lacks nesting or Van Hove singularities, orbital or spin-orbital instabilities are not competitive with the Cooper instability [11]. This suggests a superconducting region just before the MIT, which would be remarkable since the bare scattering amplitude in the Cooper channel is $U + K$, hence repulsive for $U \sim U_c \gg |K|$. We believe that this phase is analogous to the *strongly correlated superconductivity* recently identified by DMFT in a model for tetravalent alkali doped fullerenes [12]. The latter model maps by DMFT onto a threefold degenerate AIM with inverted Hund's rules, mimicking a $t \otimes H$ dynamical Jahn-Teller effect. Although different from our model (1) and (2), it contains the essential physics we have described in this work; namely, the competition between the Kondo- and an intra-impurity-screening mechanism.

We acknowledge helpful discussions with E. Tosatti. This work has been partly supported by MIUR COFIN2001 and FIRB2002, and EPSRC (U.K.).

[1] A. Georges *et al.*, Rev. Mod. Phys. **68**, 13 (1996).
[2] B. Jones and C. M. Varma, Phys. Rev. Lett. **58**, 843 (1987); B. Jones *et al.*, *ibid.* **61**, 125 (1988); B. A. Jones and C. M. Varma, Phys. Rev. B **40**, 324 (1989).
[3] I. Affleck and A. W. W. Ludwig, Phys. Rev. Lett. **68**, 1046 (1992).
[4] I. Affleck, A. W. W. Ludwig, and B. A. Jones, Phys. Rev. B **52**, 9528 (1995).
[5] All the results presented throughout refer to a fixed Kondo exchange equal to 0.05 in units of half-bandwidth, which is our unit of measure for energy.
[6] P. Nozières, J. Low Temp. Phys. **17**, 31 (1974).
[7] L. Mihály and A. Zawadowskii, J. Phys. Lett. (France) **39**, L-483 (1978).
[8] J. Gan, Phys. Rev. B **51**, 8287 (1995).
[9] G. Zaránd and J. von Delft, Phys. Rev. B **61**, 6918 (2000).
[10] Under Π^{orb}_x, $f \leftrightarrow -f$, $\Psi_f \leftrightarrow -\Psi^\dagger_f$, $\Psi_{sf} \leftrightarrow \Psi^\dagger_{sf}$, and $\Psi_c \leftrightarrow -\Psi_c$.
[11] The Bethe-Salpeter equations for bulk susceptibilities depend not only upon the irreducible vertices, which are local in DMFT, but also on products of lattice Green's functions in the appropriate particle-particle (p-p) or particle-hole (p-h) channels. While this product in the p-p channel is always singular by the Cooper phenomenon, in the p-h channels singularities may arise only due to band-structure effects. Therefore, even though local susceptibilities hence irreducible vertices are singular in p-p and p-h channels, the bulk p-p susceptibility is more likely the dominant one.
[12] M. Capone, M. Fabrizio, C. Castellani, and E. Tosatti, Science **296**, 2364 (2002).